Upper Cutoff Frequency of the Bound Wave and New Leaky Wave on the Slotline

Ján Zehentner, *Senior Member, IEEE,* Jan Macháč, and Maurizio Migliozzi

***Abstract*—Printed-circuit lines exhibit interesting behavior due to leakage of power. We have attempted to work toward a more profound understanding of uniplanar circuit properties when it comprehends planar transmission lines. Our work has focused on the slotline. We realized that the solution of its dispersion equation is multivalued. This enabled us to identify and report a new leaky wave on the slotline. The leaky wave brings down the upper cutoff frequency of the bound wave propagating over the slotline due to overlapping of the bound- and leaky-mode regions. For this case, we present some simple closed-form formulas providing this frequency limit when there is a frequency gap or when simultaneous propagation of the bound and the first or second leaky wave occurs. Propagation of the bound and leaky wave at the same time is a straightforward consequence of the multivalued nature of the solution of the dispersion equation. Evolution of the real and complex improper solutions of the equation in dependence on slotline dimensions demonstrates this clearly. We believe that conclusions drawn for the slotline also hold generally for other printed-circuit lines.**

***Index Terms*— Cutoff frequencies, electromagnetic surface waves, leaky waves, operation modes on slotlines, printed-circuit lines, slotlines.**

I. Introduction

PLANAR transmission lines used in microwave, millimeter-wave, and optical integrated circuits have been investigated intensively over the last 15 years [1]–[7]. These lines are mostly fully or partly open. Their open nature may cause leakage of power. For this reason, besides attempts to minimize natural losses, attention has been paid to leakage that can result in crosstalk between neighboring components or portions of the circuit, in lowering of their quality factors, or in outright loss of power. Leakage of power strongly depends on the cross section of the line, its dimensions, and the frequency. In any case, leakage has a significant effect on circuit performance, which can deteriorate, especially in the millimeter-wave band. We shall restrict ourselves in this paper to leakage into surface waves on the open slotline.

Shigesawa, Tsuji, and Oliner have summarized earlier investigations into effects which may occur in open printed-circuit lines and have explained in detail their comprehensive conception in [7]. Essentially, all treatises about leakage effects are based on proper integration of the matrix elements involved in the line dispersion equation having the appearance of determinant.

When speaking about leakage into surface waves on the slotline, we have to take into account earlier research results [7]. On a slotline with a relatively narrow slot, the guided dominant mode is purely bound at frequencies below the so-called spectral gap. The propagation constant of the bound wave is real. Within the spectral gap, solution of the dispersion equation is either real or complex, but in any case nonphysical. Above the spectral gap, the leaky mode can propagate, and its propagation constant is complex. Continuous increase of the slotwidth dramatically alters the dispersion curves within the spectral gap, and for a sufficiently wide slot, the bound mode and the leaky mode propagate simultaneously. Consequently, the spectral gap now disappears. The frequency band of this simultaneous propagation may be fairly wide. The recently discovered new improper real solution of the dispersion equation serves to explain continuous passing from the regime with a spectral gap to simultaneous propagation of the bound and leaky wave due to the change of slotline dimensions [6].

In this paper, we will deal with a new previously unidentified leaky wave on the slotline, with its influence on the upper limit of the dominant bound-wave frequency band, and will present closed-form formulas for this limit suitable for computer-aided design (CAD). The new leaky wave is associated with the leakage into both the TM_0 and TE_1 surface waves propagating over grounded dielectric slab. We consider our finding that this wave brings down the upper cutoff frequency of the dominant bound wave, especially on the narrow slotwidth slotline, to be a contribution to the general discussion on the characteristics of the open slotline. In this case, the regime with simultaneous propagation of the bound wave and new leaky wave dominates over the regime with the spectral gap. First of all, this concerns slotlines with lower characteristic impedance, particularly on the higher permittivity substrate. Additionally, evolution of both the real and the complex improper solutions of the dispersion equation corresponding to the new leaky wave in dependence on the slotline dimensions shows changes of the nonphysical and physical solutions. On a slotline with a wider slot, the new leaky wave has a frequency gap in which the solution is nonphysical. Physical improper complex leaky-mode solutions encompass this frequency gap on the left- and right-hand sides. The left-hand-side region of the physical improper complex solution is mostly narrow. Conclusions resulting from the solution of the dispersion equation regarding leakage into the TM_0 and TE_1 surface waves can also be extended to leakage

Manuscript received March 30, 1997; revised January 14, 1998. The work of M. Migliozzi was supported by a scholarship granted by the Faculty of Electrical Engineering, Czech Technical University, Prague, Czech Republic.

J. Zehentner and J. Macháč are with the Czech Technical University, 16627 Prague 6, Czech Republic.

M. Migliozzi is with the University of Ancona, Ancona 60131, Italy.

Publisher Item Identifier S 0018-9480(98)02729-X.

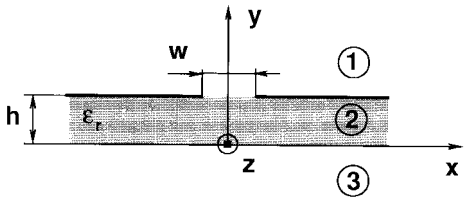

Fig. 1. Cross section of the slotline.

into the higher surface waves. Whether such leakage is worth taking into consideration is a question of each particular case, specified by the geometric and material parameters of the line. The factor that controls this thinking from the practical viewpoint is the magnitude of the frequency at which the respective leaky wave sets in. Generally, it is important to know the dispersion characteristics of planar transmission lines in order to suppress or remove their unwanted leakage while making an appropriate choice for their geometrical dimensions and material parameters.

II. The New Second Leaky Wave on the Slotline

A cross section of the investigated slotline, the denotation of its dimensions, and the placement of the axis are depicted in Fig. 1. We have analyzed the open slotline by the method of moments, modified as in the Galerkin testing procedure in the spectral domain with successive complex root searching. The integration path in the spectral domain was deformed from the real axis to include the residue contributions associated with propagation of the corresponding surface waves. The accuracy of our calculation was checked by comparing the normalized phase constant β/k_0 and the normalized leakage constant α/k_0 as a function of the normalized frequency h/λ_0, where $k_0 = \omega/c$ and $\lambda_0 = c/f$, respectively, computed for $w/h = 0.4$ and 1.0 when $\varepsilon_r = 2.25$ with their plotting first published in [8, Figs. 3, 4] and with additional relevant [7, Figs. 5, 10–16]. Within the readability of these figures, no differences were found between those results and our own. Thus, the program provides us with all solutions known and published until now [7].

Let the field be expressed in terms of the electric and magnetic Hertz vectors parallel to the y-axis and proportional to $e^{-j\gamma z}$ where γ is the propagation constant in the z-direction. Thus, corresponding electric ψ^e and magnetic ψ^m potentials describe the TM and TE fields with respect to the y-direction, superposition of which represents the total field. Taking their Fourier transforms with respect to the x-coordinate and substituting them separately into the likewise transformed Helmholtz equation, we obtain an ordinary one-dimensional wave equation. Its solution $\tilde{\psi}^e(\xi, y)$ or $\tilde{\psi}^m(\xi, y)$ is known in the spectral domain ξ. Satisfaction of the boundary conditions in the plane of the metallization results in a couple of equations which are solved by the Galerkin method. The procedure leads to a system of linear homogeneous equations for unknown amplitudes of the basis functions modeling the field within the slot. A nontrivial solution is obtained by setting its determinant to zero. The determinantal equation (known as the dispersion equation, and usually written in matrix notation), controls the dispersion characteristics of the line. The solution of this determinantal equation by a complex root-finding routine provides the propagation constant $\gamma = \beta - j\alpha$ searched for where β and α are the phase and the attenuation constant, respectively. The matrix element of dispersion equation has the form

$$\tilde{Y}_{mn} = \int_{-\infty}^{\infty} \tilde{G}_{mn}(\xi)\tilde{E}_{mi}(\xi)\tilde{E}_{nj}(\xi)\, d\xi \tag{1}$$

where $\tilde{E}_{mi}(\xi), \tilde{E}_{nj}(\xi)$ are Fourier transforms of the basis functions $E_{mi}(x,h)$, $E_{nj}(x,h)$ while m,n stand for x and/or z, and i,j distinguish particular functions from each other. We have used customary basis functions fulfilling the edge conditions in accordance with [9]. $\tilde{G}_{mn}(\xi)$ is the Green's function in a spectral domain comprising two terms. The first term corresponds to ψ^e and the latter to ψ^m potential. Both terms may have poles. In dependence on the choice of poles taken into consideration, we obtain a corresponding solution of the dispersion equation [10].

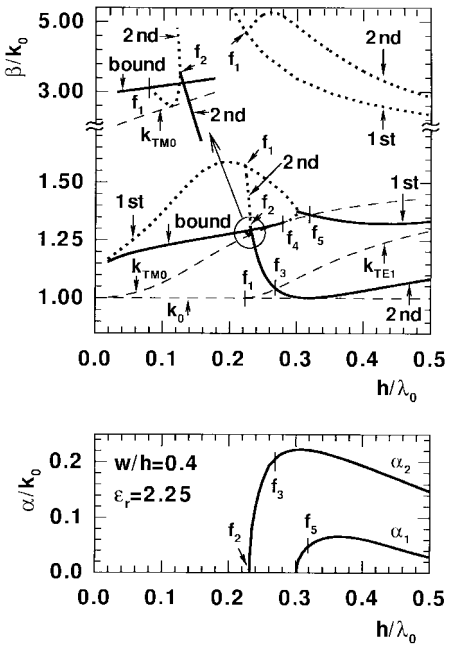

Fig. 2. The normalized phase and leakage constants for the slotline with $w/h = 0.4$ and $\varepsilon_r = 2.25$ as a function of normalized frequency (h/λ_o). (—): 1st and 2nd improper complex. (- - - -): 1st and 2nd improper real.

Several distinct situations can occur on the lossless slotline. When poles of $\tilde{G}_{mn}(\xi)$ lie only at the imaginary axis of the complex plane $\xi = \xi_r + j\xi_i$, and the integration path in $\tilde{Y}_{mn}$ is identical with the real axis, the solution of the dispersion equation is proper real and belongs to the dominant bound wave, as is seen in Fig. 2. The frequency f_4, at which the dispersion curve of the bound wave touches the curve of the TM_0 surface mode and $\beta = k_{\mathrm{TM}_0}$ determines the upper cutoff frequency of pure dominant bound-wave propagation over the slotline. The propagation constant of the TM_0 surface wave is k_{TM_0}.

When the path of integration in (1) is again equal to the real axis, but the TM_0 pole of $\tilde{G}_{mn}(\xi)$ lying at the imaginary axis is considered by its residue, the improper real solution

occurs. It starts at f_4, then grows, and later turns back to lower frequencies. The higher improper real solution, denoted in [6]–[8] as "a new improper real solution" is obtained in the same way as the first solution, but has a greater magnitude. It is the second term of a double-valued solution, the first term of which is the previous lower improper real solution. Within the spectral gap quantified by f_4 and f_5, the improper complex solution corresponding to the leaky mode splits off from the improper real solution. The pole of $\tilde{G}_{mn}(\xi)$ is now complex. Its residue contributes to the integral taken along the real axis. However, within the spectral gap the solutions are nonphysical. At frequency f_5 when β begins to be lower than k_{TM_0}, the physical improper complex solution joined with the leaky wave sets in. Integration in (1) is performed in the same way as in the preceding case.

However, besides the solutions quoted above, the dispersion equation of the slotline also has a further solution that is new and interesting. Let us denote the already known complex solution as the first leaky mode, and the new complex solution, which we are reporting here, as the second leaky mode. Subscript 1 will denote the real improper solution related with the associated TM_0 surface wave and, consequently, also with the first leaky wave. Similarly, subscript 2 will indicate quantities related with the associated TM_0 and TE_1 surface waves and with the corresponding second leaky wave.

The behavior of the second leaky wave is also illustrated in Fig. 2, and belongs to the slotline taken over from [8]. The solution for the second leaky wave is obtained when the integration path of $\tilde{Y}_{mn}$ in (1) again lies at the real axis, but both the TM_0 and the TE_1 poles of $\tilde{G}_{mn}(\xi)$, which are now complex, are accounted for in terms of their residues. This solution sets in at f_2, the frequency when the second improper complex solution splits off from the second improper real solution. The second improper real solution occurs first at frequency f_1, identical with cutoff of the TE_1 surface mode. Now the poles of $\tilde{G}_{mn}(\xi)$ are imaginary. It is seen that the second improper real solution associated with the second leaky wave breaks off from the improper real solution belonging to the first leaky wave. Then the solution goes down, crosses the bound-wave curve, and touches the phase constant line of the TM_0 surface wave. Up to this point, the imaginary poles TM_0 and TE_1 have been accounted for. Afterwards, when only the imaginary pole TE_1 is captured, the solution turns back upward and ends at the bound-wave solution, again at frequency f_1. The solutions keep their nature when passing from the first to the second leaky wave. The second higher improper real solution breaks off from the first higher improper solution again at the cutoff frequency of the TE_1 surface mode. Between f_2 and f_3, at which point the phase constant of the second leaky wave becomes equal to that of the TE_1 surface wave, the leaky wave is nonphysical in the sense of the generalized condition of leakage [11]. By chance, $f_3(0.2695)$ is here only slightly lower than $f_4(0.2780)$, the upper cutoff frequency of the pure dominant bound wave. The conventional frequency gap from f_4 to f_5 now disappears due to the presence of the second leaky wave. At frequencies higher than f_3, energy can leak into the TM_0 and TE_1 surface waves. Leakage to the TE_1 surface wave occurs at a lower angle than to the TM_0 surface wave. The corresponding leakage constant α_2 is greater than α_1.

To get a better insight into the second leaky wave, its field will be investigated in detail. The electric $\tilde{E}_y(\xi,y,z)$ and magnetic $\tilde{H}_y(\xi,y,z)$ fields perpendicular to the substrate can be written in the spectral domain in terms of two tangential electric-field components $\tilde{E}_{x0}(\xi)$, $\tilde{E}_{z0}(\xi)$ defined within the slot and specified by proper basis functions $\tilde{E}_{mi}(\xi)$, $\tilde{E}_{nj}(\xi)$, as in (1). The subscripts 1–3 now indicate the respective space, i.e., $y>h$, $0<y<h$, and $y<0$. Accordingly,

$$\tilde{E}_{y1}(\xi,y,z) = -\frac{j(\xi\tilde{E}_{x0}+\gamma\tilde{E}_{z0})}{\gamma_1}e^{-\gamma_1(y-h)}e^{-j\gamma z} \tag{2}$$

$$\tilde{H}_{y1}(\xi,y,z) = \frac{\gamma\tilde{E}_{x0}-\xi\tilde{E}_{z0}}{\omega\mu}e^{-\gamma_1(y-h)}e^{-j\gamma z} \tag{3}$$

$$\tilde{E}_{y2}(\xi,y,z) = \frac{j(\xi\tilde{E}_{x0}+\gamma\tilde{E}_{z0})}{(\gamma_2 S_2+\gamma_1\varepsilon_r C_2)\gamma_2} \cdot[\varepsilon_r\gamma_1\mathrm{sh}(\gamma_2 y)+\gamma_2\mathrm{ch}(\gamma_2 y)]e^{-j\gamma z} \tag{4}$$

$$\tilde{H}_{y2}(\xi,y,z) = \frac{\gamma\tilde{E}_{x0}-\xi\tilde{E}_{z0}}{\omega\mu(\gamma_1 S_2+\gamma_2 C_2)} \cdot[\gamma_1\mathrm{sh}(\gamma_2 y)+\gamma_2\mathrm{ch}(\gamma_2 y)]e^{-j\gamma z} \tag{5}$$

$$\tilde{E}_{y3}(\xi,y,z) = j\varepsilon_r\frac{\xi\tilde{E}_{x0}+\gamma\tilde{E}_{z0}}{\gamma_2 S_2+\gamma_1\varepsilon_r C_2}e^{\gamma_1 y}e^{-j\gamma z} \tag{6}$$

$$\tilde{H}_{y3}(\xi,y,z) = \frac{\gamma_2}{\omega\mu}\cdot\frac{\gamma\tilde{E}_{x0}-\xi\tilde{E}_{z0}}{\gamma_1 S_2+\gamma_2 C_2}e^{\gamma_1 y}e^{-j\gamma z} \tag{7}$$

where

$$S_2 = \mathrm{sh}(\gamma_2 h) \tag{8}$$

$$C_2 = \mathrm{ch}(\gamma_2 h) \tag{9}$$

$$\gamma_1^2 = \xi^2+\gamma^2-k_0^2 \tag{10}$$

$$\gamma_2^2 = \xi^2+\gamma^2-\varepsilon_r k_0^2 \tag{11}$$

and ε_r is substrate permittivity. The fields in the substrate $\tilde{E}_{y2}$, $\tilde{H}_{y2}$ and in the air $\tilde{E}_{y3}$, $\tilde{H}_{y3}$ have complex poles $\xi_{p\mathrm{TM}}$, $\xi_{p\mathrm{TE}}$ associated with ψ^m and ψ^e potentials, respectively. Their positions follow from (12) for $\xi_{p\mathrm{TM}}$ and from (13) for $\xi_{p\mathrm{TE}}$ when

$$\mathrm{th}(h\sqrt{\gamma^2+\xi_{p\mathrm{TM}}^2-\varepsilon_r k_0^2}) + \sqrt{\frac{\gamma^2+\xi_{p\mathrm{TM}}^2-\varepsilon_r k_0^2}{\gamma^2+\xi_{p\mathrm{TM}}^2-k_0^2}} = 0 \tag{12}$$

$$\mathrm{th}(h\sqrt{\gamma^2+\xi_{p\mathrm{TE}}^2-\varepsilon_r k_0^2}) + \varepsilon_r\sqrt{\frac{\gamma^2+\xi_{p\mathrm{TE}}^2-k_0^2}{\gamma^2+\xi_{p\mathrm{TE}}^2-\varepsilon_r k_0^2}} = 0. \tag{13}$$

Let us denote

$$k_{\mathrm{TM}}^2 = \gamma^2+\xi_{p\mathrm{TM}}^2 \tag{14}$$

$$k_{\mathrm{TE}}^2 = \gamma^2+\xi_{p\mathrm{TE}}^2. \tag{15}$$

After substituting (14) and (15) into (12) and (13), dispersion equations of the TM and TE surface waves propagating over a grounded dielectric slab are obtained [12]. Note that $\tilde{E}_{y1}$, $\tilde{H}_{y1}$ are poleless functions.

Far aside from the slot, the field must have the character of a surface wave. A grounded substrate supports TM and

TE modes [12]. Their propagation constants k_{TM} and k_{TE} are the common solution of (12) and (14) and (13) and (15), respectively. Assuming propagation in the z-direction, then H_x, E_y, E_z constitute TM modes while E_x, H_y, H_z constitute TE modes. Regardless of the direction of propagation, TM surface modes can be described by E_y and, similarly, H_y can describe TE surface modes.

To get the field in the space domain, the backward Fourier transform

$$E_y(x,y,z) = \frac{1}{2\pi}\int_{-\infty}^{\infty} \tilde{E}_y(\xi,y,z)e^{j\xi x}\,d\xi \tag{16}$$

of (2)–(7) is necessary. $\tilde{E}_y(\xi,y,z)$ can be decomposed into three terms as follows:

$$\tilde{E}_y(\xi,y,z) = \left[\tilde{E}_{yr}(\xi,y)+\frac{\mathrm{Res}(-\xi_p,y)}{\xi+\xi_p}+\frac{\mathrm{Res}(\xi_p,y)}{\xi-\xi_p}\right]e^{-j\gamma z} \tag{17}$$

assuming that $\tilde{E}_y(\xi,y,z)$ has only one pair of poles $\pm\xi_p$. $\tilde{E}_{yr}(\xi,y)$ is a regular function, $\mathrm{Res}(\xi_p,y)$ and $\mathrm{Res}(-\xi_p,y)$ are residues of the function $\tilde{E}_y(\xi,y)$ at the poles $\pm\xi_p$ and at a given position y.

Poles ξ_p are either complex or imaginary. Let us substitute (17) into (16). Integration in (16) along the real axis in the ξ plane results in the field always decaying with increasing $|x|$, i.e., we get the bound wave. To get an improper wave with increasing amplitude in the $\pm x$-direction, the integration path must be modified, as seen in the contour C in Fig. 3(a) and (b). Now

$$\begin{aligned} E_y(x,y,z) &= \frac{1}{2\pi}\int_C \tilde{E}_y(\xi,y,z)e^{j\xi x}\,d\xi \\ &= \left\{\frac{1}{2\pi}\int_{-\infty}^{\infty}\tilde{E}_{yr}(\xi,y)e^{j\xi x}\,d\xi + j\,\mathrm{sgn}(x)\right. \\ &\qquad \left.\cdot\left[\mathrm{Res}(-\xi_p,y)e^{-j\xi_p x}+\mathrm{Res}(\xi_p,y)e^{j\xi_p x}\right]\right\}e^{-j\gamma z}. \end{aligned} \tag{18}$$

The first term provides the bound wave whereas the second term represents the superposition of two waves. One of them with decreasing and the second one with growing amplitude when $|x|$ tends to infinity. The latter is an improper wave since it does not fulfill the radiation condition at infinity. Far from the slot, the field can be approximated by a wave

$$E_{yR} = j\,\mathrm{Res}(-\xi_p,y)e^{-j\xi_p x}e^{-j\gamma z} \tag{19}$$

propagating obliquely to the right from the slot and by another wave

$$E_{yL} = -j\,\mathrm{Res}(\xi_p,y)e^{j\xi_p x}e^{-j\gamma z} \tag{20}$$

propagating obliquely to the left from the slot. Their propagation constants in the x-direction are equal to the pole location $\pm\xi_p$. Propagation constants $\xi_p = \xi_{pr}+j\xi_{pi}$ and $\gamma = \beta - j\alpha$ are complex. Let us denote k_s as k_{TM} or k_{TE}, which for a lossless substrate is real. After decomposition and rearrangement, (14) and (15) gives

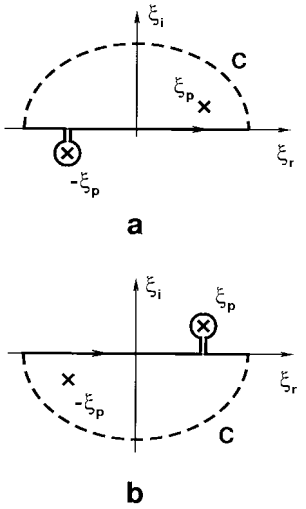

Fig. 3. Integration path for (18) in the plane ξ.

$$\beta^2+\xi_{pr}^2 = k_s^2+\alpha^2+\xi_{pi}^2 \tag{21}$$

$$\alpha\beta = \xi_{pr}\xi_{pi}. \tag{22}$$

The phase constant of E_{yR} and E_{yL} in the z- and x-directions is β and ξ_{pr}, respectively, so that the phase constant in the direction of their propagation is

$$k_p = \sqrt{\beta^2+\xi_{pr}^2} = \sqrt{k_s^2+\alpha^2+\xi_{pi}^2}. \tag{23}$$

Both these waves propagate at angle Θ read from the z-axis

$$\Theta = \arctan(\xi_{pr}/\beta) = \arccos(\beta/\sqrt{k_s^2+\alpha^2+\xi_{pi}^2}). \tag{24}$$

Equation (24) removes the approximation sign in [4, eq. (2)]. Mostly α and ξ_{pi} are considerably less than k_s. Consequently, the difference between Θ calculated according to (24) and according to [4, eq. (2)] is insignificant. However, for our examples shown in Figs. 4, 7, and 8, this difference amounts to 0.60°, 0.74°, and 1.66°, respectively. Readability in the original larger size figures is better than 0.5°. Thus, the transversal field distribution shown in Figs. 4, 7, and 8 confirms the validity of (24). The idea quoted above holds analogously for $H_y(x,y,z)$.

$\tilde{E}_{y2}(\xi,y,z)$ with complex poles $\pm\xi_{p\mathrm{TM}}$ represents a leaky wave that at a great distance from the slot continuously modifies and passes on the TM surface wave. Similarly, $\tilde{H}_{y2}(\xi,y,z)$ has poles $\pm\xi_{p\mathrm{TE}}$ and passes on the TE surface wave when is sufficiently far away from the slot. On the other hand, $\tilde{E}_{y1}(\xi,y,z)$ and $\tilde{H}_{y1}(\xi,y,z)$ have no poles. Consequently, this field decays in any case with growing $|x|$ since the metallization screens the field on its opposite side.

A theoretical reason for an existence of the first leaky wave has been given above. It is related with the poles $\pm\xi_{p\mathrm{TM}_0}$ corresponding to the TM_0 surface mode. It leaks at an angle

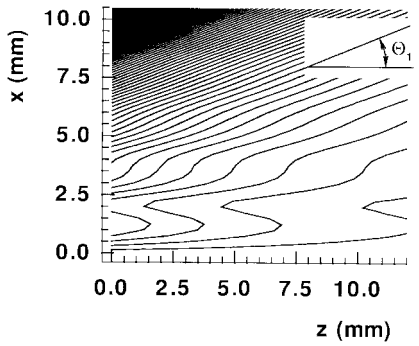

Fig. 4. The first leaky-wave contour lines of the electric-field component E_{y2} perpendicular to the substrate surface $y = 0$ plotted in the xz-plane for the slotline with $w/h = 0.5$, $\varepsilon_r = 2.25$, and $h/\lambda_o = 0.45$. Θ_1 is the angle of leakage.

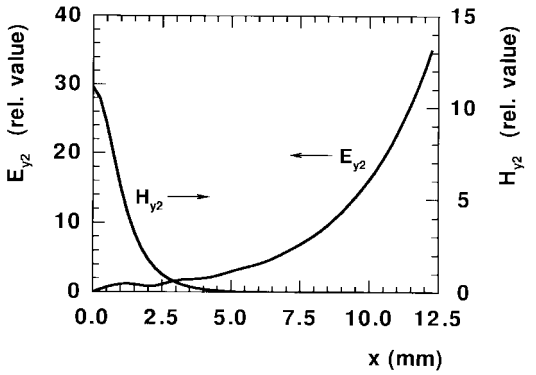

Fig. 5. The first leaky-wave components of the electric E_{y2} and magnetic H_{y2} field perpendicular to the substrate surface $y = 0$ in the plane $z = 0$ for the same slotline as in Fig. 4.

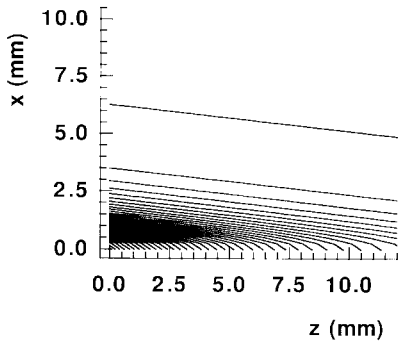

Fig. 6. The first leaky-wave contour lines of the magnetic field component H_{y2} perpendicular to the substrate surface $y = 0$ plotted in the xz-plane for the same slotline as in Fig. 4.

Θ_1 according to (24) where $k_s = k_{\mathrm{TM}_0}$. The contour plot of its electric field perpendicular to the substrate surface $y = 0$ is shown in Fig. 4. The greater the line density, the higher the field strength. Since $\xi_{p\mathrm{TM}_0}$ is the pole of $\tilde{E}_{y2}$, and not the pole of $\tilde{H}_{y2}$, the component H_{y2}, perpendicular to the substrate surface, decreases with growing $|x|$, as is seen in Fig. 5, and as documented again by the contour plot in Fig. 6.

As we have mentioned above, the second leaky wave occurs when poles related to ψ^e and ψ^m potentials, i.e., $\xi_{p\mathrm{TM}_0}$

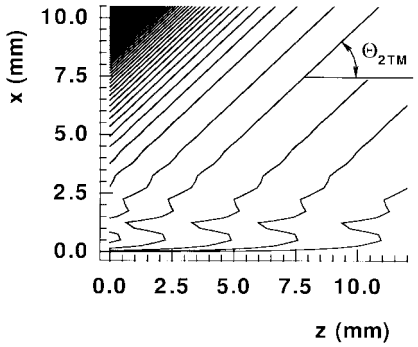

Fig. 7. Contour lines of E_{y2} similar to those in Fig. 4, but now for the second leaky wave on the same slotline.

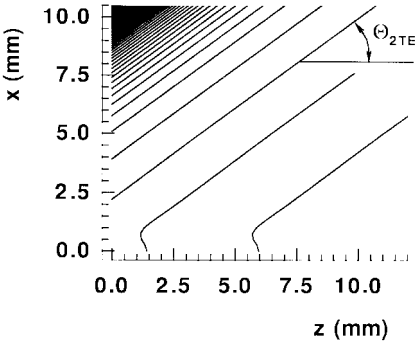

Fig. 8. The second leaky-wave contour lines of H_{y2} perpendicular to the substrate surface $y = 0$ plotted in the xz-plane for the same slotline as in Fig. 4.

and $\xi_{p\mathrm{TE}_1}$, are taken into consideration. Besides the bound term, the total field consists of the TM_0 and TE_1 surface waves. They both have the same propagation constant γ in the z-direction, but different propagation constants in the x-direction. Their amplitudes are proportional to the residues at the $\xi_{p\mathrm{TM}_0}$ and $\xi_{p\mathrm{TE}_1}$ poles. The corresponding angles of propagation also differ as follows:

$$\Theta_{2\mathrm{TM}} = \arccos(\beta/\sqrt{k_{\mathrm{TM}_0}^2 + \alpha^2 + \xi_{p\mathrm{TM}_0 i}^2}) \qquad (25)$$

$$\Theta_{2\mathrm{TE}} = \arccos(\beta/\sqrt{k_{\mathrm{TE}_1}^2 + \alpha^2 + \xi_{p\mathrm{TE}_1 i}^2}) \qquad (26)$$

as is seen in the contour plots in Figs. 7 and 8. The magnitudes of these angles agree with those read in Figs. 7 and 8 when leakage constant α is accounted for in (25) and (26). Fig. 9 confirms a feeling that now both TM_0 and TE_1 surface waves could occur far away from the slot.

When w/h increases (e.g., to 0.5), f_3 is distinctly lower than f_4 (see Fig. 10), and within the frequency gap from f_6 to f_7 the phase constant of the second leaky wave is lower than k_0. Here, the solution is nonphysical since β does not comply with the generalized condition of leakage [11]. Now the influence of the first leaky wave can assert itself. Above the frequency gap, i.e., above f_7, the second leaky wave is again physical and may exist simultaneously with the first leaky wave.

The newly revealed characteristics of the second leaky wave are more expressive on the higher permittivity substrate,

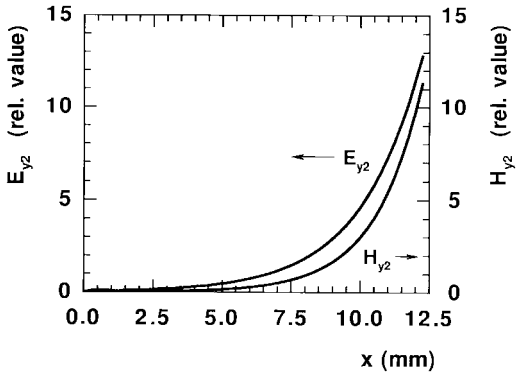

Fig. 9. A plot of the electric E_{y2} and magnetic H_{y2} field components of the second leaky wave perpendicular to the substrate surface $y = 0$ in the plane $z = 0$ similar to that in Fig. 5 for the same slotline as in Fig. 4.

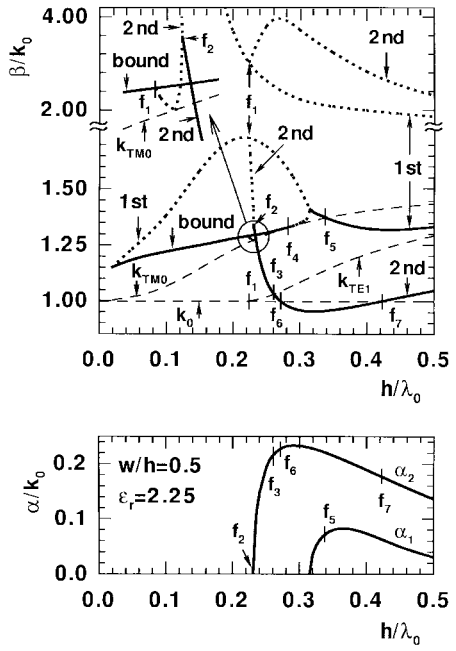

Fig. 10. A plot similar to that in Fig. 2, but for a wider slotwidth $w/h = 0.5$. (—): 1st and 2nd improper complex. (- - - -): 1st and 2nd improper real.

e.g., when $\varepsilon_r = 10.8$, $w/h = 0.236$ ($w = 0.15$ mm and $h = 0.635$ mm) (see Fig. 11). Now the overlapping interval of simultaneous propagation of the bound and the second leaky wave from $f_3 = 46.0$ GHz to $f_4 = 59.9$ GHz is sufficiently significant for practical purposes. The second leaky wave has much greater influence on the behavior of the slotline of a narrower slotwidth (see Figs. 2, 11), while for a wider slotwidth its influence is negligible since f_3 and f_6 are too close together (see Figs. 10 and 12–15).

III. Dependence of Second Leaky-Wave Solutions on Slotline Dimensions

It is interesting to observe how the dispersion characteristics of the second leaky wave change with the normalized slotline dimension w/h. Their coupling to characteristics of the first leaky wave at and above the cutoff frequency of the TE_1

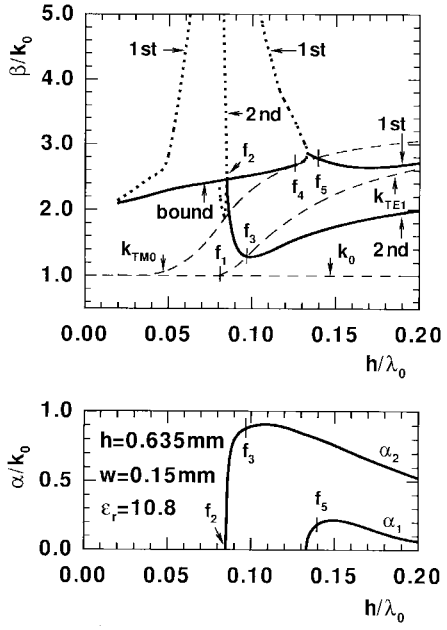

Fig. 11. A plot similar to that in Fig. 2, but for a narrower slotwidth $w/h = 0.236$ and higher substrate permittivity $\varepsilon_r = 10.8$. (—): 1st and 2nd improper complex. (- - - -): 1st and 2nd improper real.

surface wave demonstrates the multivalued nature and the completeness of the solution of the dispersion equation.

The dispersion characteristics of a slotline vary with increasing relative dimension w/h. The sequence of charts in Figs. 2, 10, and 12–15 demonstrates this objectively. Their common feature is that the second solution (either improper real or improper complex) always sets in at f_1, the cutoff frequency of the TE_1 surface wave, and has the same value as the first solution at this splitoff point. When the solution associated with the first leaky wave has an improper real solution at frequency f_1, the second solution also breaks away like the improper real (see Figs. 2, 12, and 13). Similarly, the improper complex solution of the second leaky mode splits off from the complex solution of the first leaky wave, i.e., this concerns both the phase and leakage constant (see Figs. 14 and 15).

Figs. 10 and 12–15 give evidence that the second leaky wave does not make itself useful on wide slotwidth slotlines. The first leaky wave dominates and controls their dispersion characteristics. A narrow slot offers a greater chance to excite the second leaky wave, as in Fig. 2 and 11. This particularly concerns circuits made on higher permittivity substrates.

Transition from the regime with the spectral gap to simultaneous propagation of the bound wave and the first leaky wave radiating into the TM_0 surface wave (which has a zero cutoff frequency) is explained in [6] and [7] in terms of occurrence of the same number of solutions of the dispersion equation at all frequencies. However, the same account is not applicable in the case of the second leaky mode, the presence of which is possible only above f_1, the nonzero cutoff frequency of the TE_1 surface wave. When f_1 is crossed toward higher frequencies and the second leaky mode is considered, the total number of solutions doubles in comparison with the case when only the first leaky mode is taken into account. This figure holds up to the TM_1 cutoff frequency, above which the total

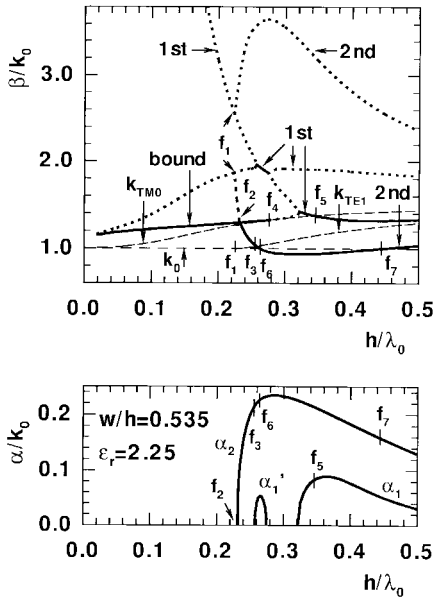

Fig. 12. A plot similar to that in Fig. 10, but for a wider slotwidth $w/h = 0.535$. (—): 1st and 2nd improper complex. (- - - -): 1st and 2nd improper real.

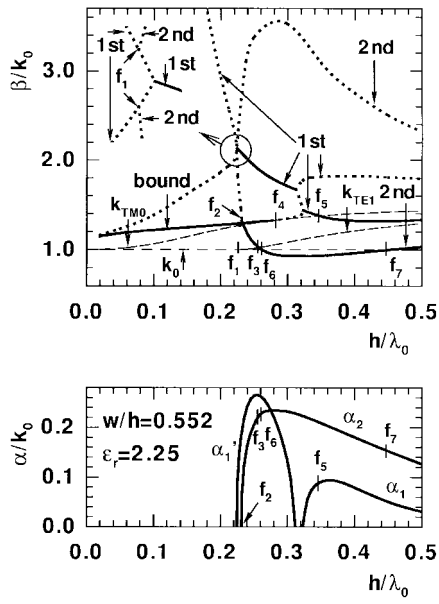

Fig. 13. A plot similar to that in Fig. 12, but for a slightly wider slotwidth $w/h = 0.552$. (—): 1st and 2nd improper complex. (- - - -): 1st and 2nd improper real.

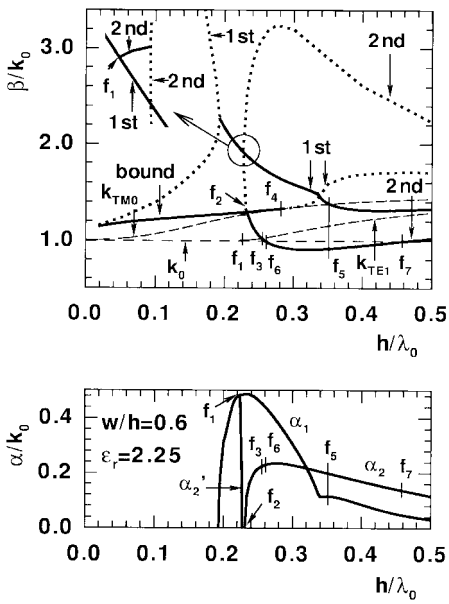

Fig. 14. A plot similar to that in Fig. 13, but for a slotwidth increased to $w/h = 0.6$. (—): 1st and 2nd improper complex. (- - - -): 1st and 2nd improper real.

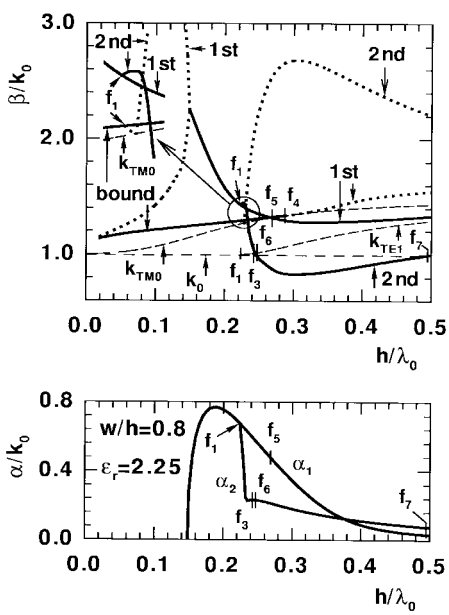

Fig. 15. A plot similar to that in Fig. 14, but for a very wide slot with $w/h = 0.8$. (—): 1st and 2nd improper complex. (- - - -): 1st and 2nd improper real.

number of solutions again doubles in comparison with the number of solutions below this frequency. In principle, the dispersion equation can provide additional solutions associated with TM_1, TE_2, etc., surface modes. Unfortunately, their cutoff frequencies are very high. Therefore, application of the slotline at such frequencies would be senseless.

IV. Upper Cutoff Frequency of the Bound Wave

A role that the first and the second leaky waves play on the slotline has been shown in Section II. Basically, if excited they limit the frequency band in which only the bound wave propagates. To avoid the trouble caused by surface leakage, it is necessary to know the upper frequency cutoff of the dominant bound wave. In case of a spectral gap, this is given by f_4 in Figs. 2 and 11–14, and denoted hereafter as f_c. When simultaneous propagation of the bound wave and the first leaky wave occurs, the upper frequency cutoff f_{c1} is equal to f_5, as shown in Fig. 15. If the regions of the bound and the second leaky waves overlap, the cutoff frequency f_{c2} is given by f_3 (e.g., Figs. 2, 10, 11).

The normalized upper frequency cutoff (h/λ_c) instead of f_c depending on the relative dimension w/h and permittivity

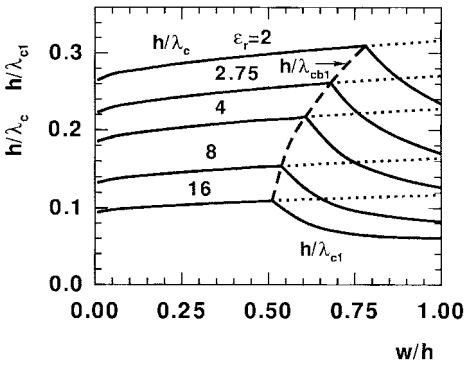

Fig. 16. The normalized upper frequency cutoff of the dominant bound wave determined by the spectral gap (h/λ_c) and by simultaneous propagation of the first leaky wave (h/λ_{c1}).

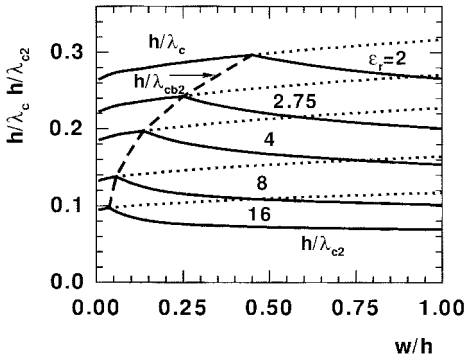

Fig. 17. A plot similar to that in Fig. 16, but the normalized upper frequency cutoff of the dominant bound wave (h/λ_{c2}) is now determined by simultaneous propagation of the second leaky wave.

ε_r is shown in Fig. 16. The figure is based on a set of data calculated for various w/h and ε_r combinations. Their subsequent manipulation by the least-squares method results in the closed-form formula

$$(h/\lambda_c) = A_1[A_2 + A_3(w/h)^{A_4}]^{A_5} \tag{27}$$

where

$$A_1 = 1 + 0.045e^{-0.05|\varepsilon_r - 9|^{2.5}} \tag{28}$$

$$A_2 = 0.272\,51e^{-0.285\,29\varepsilon_r} + 0.176\,45 \tag{29}$$

$$A_3 = (0.939\,85 - 0.003\,688\,9\varepsilon_r^{0.580\,52})^{41.995} \tag{30}$$

$$A_4 = (0.742 - 0.0064\varepsilon_r^{0.375})^{1.94} \tag{31}$$

$$A_5 = (1.0031 + 0.026\,035\varepsilon_r^{0.220\,43})^{6.2803} \tag{32}$$

are simple functions of ε_r. Equations (27)–(32) hold when $0.01 \le w/h \le 1$ and $2 \le \varepsilon_r \le 16$.

The following equation:

$$(h/\lambda_{cb1}) = [0.76388 + 0.20999(w/h - 0.493)^{0.08212}]^{24.589} \tag{33}$$

satisfies the condition $f_c = f_{c1}$ and controls the boundary line separating the left pure bound-wave region from the right region of simultaneous propagation of the bound wave and the first leaky wave.

Similarly, the normalized frequency (h/λ_{c1}) instead of f_{c1} is also plotted in Fig. 16. The formula

$$(h/\lambda_{c1}) = [B_1 + B_2(w/h)^{-B_3}]^2 \tag{34}$$

describes f_{c1}. B_1, B_2, B_3, the ε_r dependent functions, are as follows:

$$B_1 = \varepsilon_r/(1.85 + 1.44\varepsilon_r^{1.375}) - 0.024e^{-0.065|\varepsilon_r - 6.5|^2} \tag{35}$$

$$B_2 = (0.002 + 0.5/\varepsilon_r^{2.12})^{0.92} - 0.011e^{-0.2|\varepsilon_r - 2.75|^{2.5}} \tag{36}$$

$$B_3 = 2.59(\varepsilon_r - 1.75)^{0.25} - 0.86e^{-0.0075|\varepsilon_r - 18|^{2.04}} - 0.08e^{-0.1|\varepsilon_r - 8|^2}. \tag{37}$$

Equations (34)–(37) have the same interval of validity as (27).

The condition $f_c = f_{c2}$ produces the equation

$$(h/\lambda_{cb2}) = [0.0081636 + 0.14095(w/h - 0.037)^{0.68218}]^{0.49415} \tag{38}$$

defining the boundary line separating the left pure bound-wave region from the right region of simultaneous propagation of the bound and the second leaky waves (see Fig. 17).

The normalized upper frequency cutoff (h/λ_{c2}) instead of f_{c2} is also drawn in Fig. 17 and

$$(h/\lambda_{c2}) = [C_1 + C_2(w/h)^{-C_3}]^{C_4} + C_5 \tag{39}$$

where

$$C_1 = (\varepsilon_r - 1.928)^{0.899}/(2.0 + 1.2\varepsilon_r^{1.3}) + 0.01e^{-1.3|\varepsilon_r - 3.2|^{3.0}} \tag{40}$$

$$C_2 = 2.325/\varepsilon_r^{1.732} - 0.043e^{-0.5|\varepsilon_r - 3.3|^{4.0}} - 0.008e^{-0.09|\varepsilon_r - 6.5|^{3.0}} - 0.01e^{-15.0|\varepsilon_r - 4.7|^{3.0}} + 0.01e^{-|\varepsilon_r - 4.0|^{10.0}} \tag{41}$$

$$C_3 = 0.0794(\varepsilon_r - 1.73)^{0.605} - 0.012e^{-0.03|\varepsilon_r - 8.0|^{2.5}} \tag{42}$$

$$C_4 = 1.95 + 75.0/\varepsilon_r^{5.2} \tag{43}$$

$$C_5 = 0.012e^{-10.0|\varepsilon_r - 2.0|^{7.0}}. \tag{44}$$

Equations (39)–(44) hold when w/h and ε_r lie in the same intervals as they do for (27). Formulas (27)–(44) can easily be implemented into CAD. They determine the desired operation frequency band in which only the bound wave can propagate.

V. Conclusions

We have reported the discovery of a new previously unidentified leaky wave on the slotline. Its occurrence is a direct consequence of the multivalued nature of the solution of the dispersion equation with respect to individual surface waves supported by a grounded dielectric slab. This new second leaky wave is associated with leakage into the TM_0 and TE_1 surface waves. Their directions of propagation differ. We have presented plots of contour lines for the already known first leaky wave and also for the new second leaky wave. They confirm the correct value of the angle at which a particular leaky wave radiates from the slot when both its propagation and leakage constants are taken into account in the calculation. Their influence is more expressive for the second than for the first leaky wave. The second leaky

wave has greater significance on slotlines with a narrower slotwidth and made on a higher permittivity substrate. Then simultaneous propagation of the bound and the second leaky waves occurs. This fact reduces the usable frequency band of pure bound-wave propagation. On a slotline with a wider slotwidth, the role of the first leaky wave is predominant. Now the second leaky wave exhibits a frequency gap in which its improper complex solution is nonphysical. However, above this frequency gap, simultaneous propagation of the first and second leaky wave is possible. The second leaky wave brings down the upper cutoff frequency of pure bound-wave propagation. We have, therefore, presented closed-form formulas useful for CAD providing this frequency limit. They facilitate determination of the desired operation frequency band. Discussion of the dispersion characteristics of the second leaky wave gives better insight into the mechanism of the wave processes taking place on the slotline. We believe that the new effects revealed on the slotline may occur on other open printed-circuit lines and possess generality encoded in the multivalued solution of their dispersion equation.

ACKNOWLEDGMENT

This work was done on the SP-2 computer at the Joint Supercomputer Center, Czech Technical University, Prague, Czech Republic, University of Chemical Technology, Prague, Czech Republic, and IBM Prague, Prague, Czech Republic.

REFERENCES

[1] A. A. Oliner, "Leakage from various waveguides in millimeter wave circuits," *Radio Sci.*, vol. 22, pp. 866–872, Nov. 1987.
[2] D. R. Jackson and A. A. Oliner, "A leaky-wave analysis of the high-gain printed antenna configuration," *IEEE Trans. Antennas Propagat.*, vol. 36, pp. 905–910, July 1988.
[3] N. K. Das and D. M. Pozar, "Full-wave spectral-domain computation of material, radiation, and guided wave losses in infinite multilayered printed transmission lines," *IEEE Trans. Microwave Theory Tech.*, vol. 39, pp. 54–63, Jan. 1991.
[4] H. Shigesawa, M. Tsuji, and A. A. Oliner, "Dominant mode power leakage from printed-circuit waveguides," *Radio Sci.*, vol. 26, pp. 559–564, Mar.-Apr. 1991.
[5] M. Tsuji, H. Shigesawa, and A. A. Oliner, "Simultaneous propagation of both bound and leaky dominant modes on conductor-backed coplanar strips," in *IEEE MTT-S Int. Microwave Symp. Dig.*, Atlanta, GA, June 1993, pp. 1295–1298.
[6] H. Shigesawa, M. Tsuji, and A. A. Oliner, "Evolution of new nonspectral real solution and its role in explaining the simultaneous propagation of both bound and leaky dominant modes on printed-circuit lines," in *Proc. Int. Symp. Electromagnetic Theory*, St. Petersburg, Russia, May 1995, pp. 773–775.
[7] ——, "Simultaneous propagation of bound and leaky dominant modes on printed-circuit lines: A new general effect," *IEEE Trans. Microwave Theory Tech.*, vol. 43, pp. 3007–3019, Dec. 1995.
[8] ——, "Simultaneous propagation of bound and leaky dominant modes on printed-circuit lines: A new general effect," in *IEEE MTT-S Int. Microwave Symp. Dig.*, Orlando, FL, May 1995, pp. 145–148.
[9] T. Itoh, *Numerical Techniques for Microwave and Millimeter-Wave Passive Structures.* New York: Wiley, 1989, p. 352.
[10] D. Nghiem, J. T. Williams, D. R. Jackson, and A. A. Oliner, "Proper and improper dominant mode solutions for a stripline with an air gap," *Radio Sci.*, vol. 28, pp. 1163–1180, Nov.–Dec. 1993.
[11] D. Nghiem, J. T. Williams, D. R. Jackson, and K. Michalski, "The choice of integration path in the spectral-domain solution of leaky modes," Personal communication about the viewgraphs presented at the URSI Nat. Radio Sci. Meeting, Boulder, CO, Jan. 1995.
[12] R. E. Collin, *Field Theory of Guided Waves*, 2nd ed. New York: IEEE Press, 1991, p. 732.

Ján Zehentner (M'92–SM'96) received the M.Sc. degree from the Czech Technical University (CTU), Prague, Czech Republic, in 1962, the Ph.D. degree from the Czechoslovak Academy of Sciences, Prague, Czech Republic, in 1972, both in radioelectronics engineering, and the Dr.Sc. degree in radioelectronics from CTU, in 1991.

He has been with the Faculty of Electrical Engineering, CTU, as an Assistant Professor (1963-1979), Associate Professor (1980-1993), and since 1994, a Professor of radioelectronics. He is engaged in teaching and research in electromagnetic-field theory, and microwave and millimeter-wave theory and techniques, particularly in microwave integrated circuits. He has been the Contractor for three European Union (EU) European Commission, Brussels, Belgium, and two university projects dealing with uniplanar circuits and teaching of microwave engineering. In the course of these projects, he spent some time at the universities of Ulm, Ancona, and Leeds. He has authored and co-authored over 60 technical papers in journals and conference proceedings, 4 textbooks, and holds 7 patents.

Prof. Zehentner is a member of the Czech Electrical Society and the State Radioelectronics Thesis Defence Commission for both the Ph.D. and the Dr.Sc. degrees. He is currently Head of the Czech Electrical Society Professional Group on Microwave Technology. From 1991 to 1994, he was a member of the Scientific Council of the Faculty of Electrical Engineering, CTU. He has served as a member of the editorial boards of the *Journal of Electrical Engineering*, *Electronic Horizon*, and the IEEE TRANSACTIONS ON MICROWAVE THEORY AND TECHNIQUES. He has participated in the organization of all Czechoslovak Microwave Conferences in the Steering and Technical Programme Committees. He has been a member of the Management and Technical Programme Committees of European Microwave Conferences (EuMC), and chaired the 26th EuMC.

Jan Macháč received the M.Sc. degree in electronics from the Czech Technical University (CTU), Prague, Czech Republic, in 1977, the Ph.D. degree in electronics from Institute of Radioengineering and Electronics, Czechoslovak Academy of Sciences, Prague, Czech Republic, in 1982, and the Dr.Sc. degree in readioelectronics from CTU in 1996.

From 1977 to 1984, he was with the Institute of Radioengineering and Electronics, Czechoslovak Academy of Sciences, where he worked on semiconductor sources and detectors of light radiation. In 1984, he joined the Faculty of Electrical Engineering, CTU, where he was Assistant Professor until 1991, and is currently an Associate Professor of electrical engineering. He is engaged in teaching electromagnetic-field theory and numerical methods for studying electromagnetic fields. His main research interests are modeling of planar passive elements and subsystems used in millimeter-wave techniques and field theory. He was a contractor for one European Union (EU) European Commission project, and for one university project dealing with the study of electromagnetic fields by numerical methods. Under the EU project, he spend five months at the University of Ulm. In 1990, he was a member of the Organizing Committee of the URSI General Assembly. Since 1995, he has been a member of the Technical Programme Committee of the European Microwave Conference, and was the conference secretary in 1996. He has authored and co-authored over 60 scientific papers in journals and conference proceedings and one textbook.

Dr. Macháč is a member of the Czech Electrical Society.

Maurizio Migliozzi received the M.Sc. degree in electronics engineering (graduating with distinction) from the University of Ancona, Ancona, Italy, in 1997.

In 1996, he spent six months at the Czech Technical University (CTU), Prague, Czech Republic. His research interest is mainly in the area of planar microwave transmission lines.